

EXPERIMENTAL AND NUMERICAL ANALYSIS OF VICKERS HARDNESS TESTING

Evando E. Medeiros¹ & Avelino M.S. Dias^{2,*}

¹P+Z Engineering GmbH, Anton Ditt Bogen 3 - Munich, Germany

evandomedeiros@gmail.com

²Federal University of Rio Grande do Norte (UFRN), University Campus, 59072-870, Natal, Brazil

avelino.dias@ct.ufrn.br

ABSTRACT

Indentation Tests have been largely used for determination of superficial hardness. Due to its great applicability, new methodologies are being developed in order to determine mechanical properties such as Young Modulus (E) and fracture toughness (K_{IC}) for brittle materials. However, the Vickers indentation has several limitations and complications as methodology for characterization of these material properties. Thus, the use of a numerical technique able to determine fields of stress and strain during the indentation cycle may give a more reliable interpretation of this kind of test. Hence, this work aims to study the mechanical behaviour of a specimen of tungsten carbide cobalt (WC-Co) during a Vickers indentation test, based on FE calculations with the commercial solver MSC Marc. In a future development of this work, it will be developed numerical models to simulate the mechanisms of crack onset and their propagation during the tests.

Keywords: *Finite Element, Contact, Hardness Testing, Fracture Mechanics*

1. INTRODUCTION

One of the first cases relating to the study of the problem of material failure date back to the 15th century with some experiments of Leonardo da Vinci. In these studies, Da Vinci results showed that the resistance of wires varies inversely to the length of the wire. Leonardo interpreted this behaviour correctly by linking it to the higher probability of internal defects for longer wires [1]. In 1920, Griffith performed a stress analysis to study a plate with elliptical holes. By applying the First Law of Thermodynamics, he formulated a theory for crack propagation based on the energy balance. The Griffith's model predicted correctly the relationship between the resistance and the crack length in specimens of glass, but failed when applied to metals. In 1948, Irwin and Orowan, independently, proposed a modification to this model, extending the analysis to metals [1]. The tragedy of the Liberty ships during World War II, highlighted the need of better comprehension and models able to predict failures as well to establish predictive methodologies to prevent the collapse of structures. Several parameters, such as K_{IC} , $CTOD$, G -Energy or J Integral, were developed as an attempt to measure the resistance to crack growth. The determination of K_{IC} seems adequate, as failure criterion, since it satisfies the criteria of validity of Linear Elastic Fracture Mechanics (LEFM). The motivation for the use of such specimens with long cracks is that the plasticity is restricted to the crack tip and the validity of the LEFM is ensured. So long the tri-axial stress state ahead of the crack meets the restricted flow conditions, commonly called SSY (small scale yield) conditions, the LEFM theory can be assessed in structural engineering using data from laboratory specimens [2]. Usually, conventional tests for fracture toughness measurement uses specimens with deep cracks, such as SENB (Specimen Edge Notched Bend) and CT (Compact Specimen), as illustrated in Figure 1.

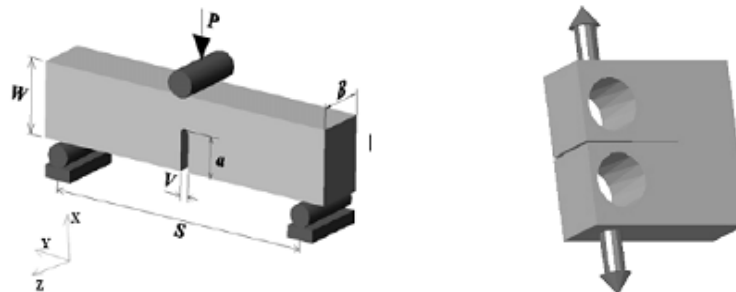


Figure 1. Common specimen, SENB (Single edge notched bend) and CT (Compact specimen), respectively.

Sometimes the manufacturing of conventional specimens for fracture tests can be a hard task, especially for materials with peculiar characteristics such as the WC-Co alloys, which have very high surface hardness and slightly

elastic-plastic stress-strain response [3, 4]. Therefore, some authors are developing methodologies based on non-conventional tests and in order to determine mechanical properties of such materials.

One field of interest for these studies is the determination of fracture toughness for WC-Co alloys based on Indentation tests. Recently, several models have been developed in order to incorporate LEFM concepts to these tests in order to evaluate wear, erosion, and also fracture toughness K_{IC} for brittle materials. Table 1 summarizes some advantages and complications of this method [3].

Table 1: Vickers Indentation on Determination of Fracture Toughness - Advantages and Limitations

Advantages	Limitations
1. Vickers Test equipments are commonly found in research laboratories	1. Measurement are not accurate
2. Preparation of specimen is relatively simple	2. Several mechanisms of crack nucleation and propagation;
3. The test is quick, cheap and it can be classified as non-destructive	3. Literature reports diverse equations for K_{IC}

In order to avoid discrepancies on the Indentation results, the comprehension of the mechanism of crack nucleation and growth as well the most adequate semi-empirical model to be assessed is an important requirement. In this sense, the use of a numerical technique able to determine fields of stress and strain may assist in a more reliable interpretation [6]. The purpose of this work is to develop FE models able to characterize the stress fields during the loading phase Indentation test. The FE simulations are based on a contact problem between rigid indenter and the WC-Co specimen, modeled with solid elements. It is expected that with these numerical models, it may be possible to better identify and understand the mechanisms of nucleation and propagation of cracks that occur during these tests.

2. VICKERS HARDNESS TESTING

Indentation tests consist of compressing slowly a hard indenter on a specimen during a certain time interval. The test for Hardness Vickers (H) is characterized by a diamond pyramid indenter with an angle of opening between the faces 136° . The Hardness is defined as the ratio between the applied force and the print area eq. (1) [3].

$$H = \frac{F}{A} = \frac{2 F \sin(136^\circ / 2)}{d^2} \quad (1)$$

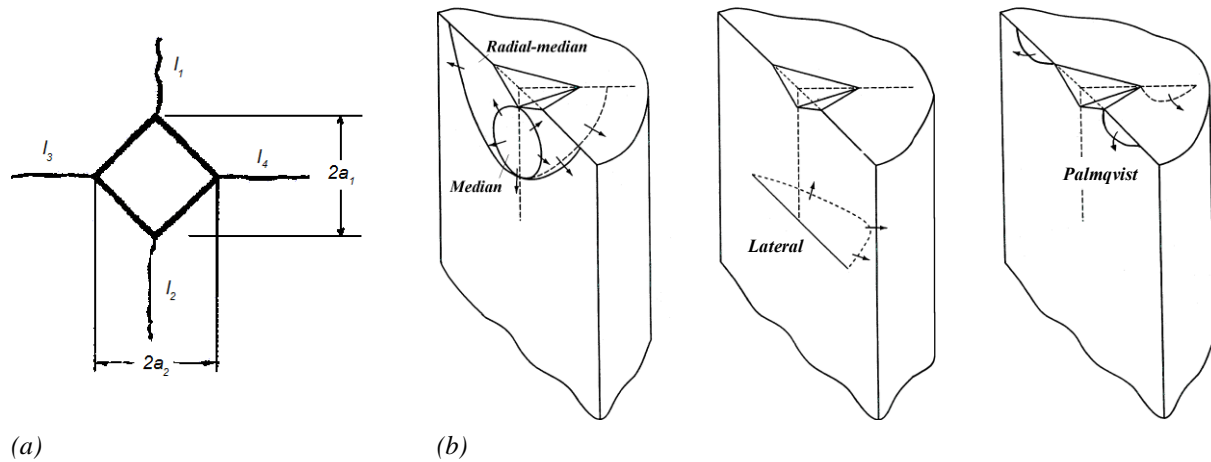
The introduction of the force F creates a high stress level and induces plastic stresses in the specimen during the loading phase. When the load is removed (unloading phase), a relaxation of the elastic strains occurs and residual stresses are induced on this region. In brittle specimens, radial cracks nucleate on the corners of the indent print, in order to re-establish the mechanical equilibrium material, and propagates on the direction of the indent diagonal. The fracture toughness K_{IC} can be correlated with the length of radial cracks. The mechanism of nucleation and propagation of radial cracks during the indentation test is dependent on the material properties, grain size and shape of the indenter. The main mechanisms of nucleation are generally described in the literature as Median, Lateral, Radial and Palmqvist, as illustrated in Figure 2 and Figure 3 [7-8].

2.1. Mechanism of crack nucleation during Indentation

Radial cracks have mainly three mechanism of nucleation, median or Palmqvist or a combination of both (Figure 4). The radial crack in the surface of the sample is visible and measurable; it has become an important parameter for evaluating the fracture toughness of the material tested. Some researchers determined semi-empirical correlations among the radial crack length, hardness, Young Modulus, fracture toughness, etc [3].

2.1.1. The median crack

During the loading phase, a hydrostatic stress field under the hardness print appears. This stress field would be responsible for the nucleation of the crack in the interface between plastic and elastic regions. As the applied load increases, the crack propagates stably until P reaches a critical value. From this critical load, an unstable propagation occurs and radial cracks appear on the sample surface. Alternatively, the nucleation and propagation can occur during the unloading phase, even if the test load is less than the critical value. In this case, the stress σ_3 , (Figure 3b) is tensile due to the relaxation of elastic stress and plastic deformation in the region of indentation [3].



(a) (b)
 Figure 2. (a) Radial cracks near to the hardness print (b) Mechanisms of crack nucleation during Indentation[5, 8]

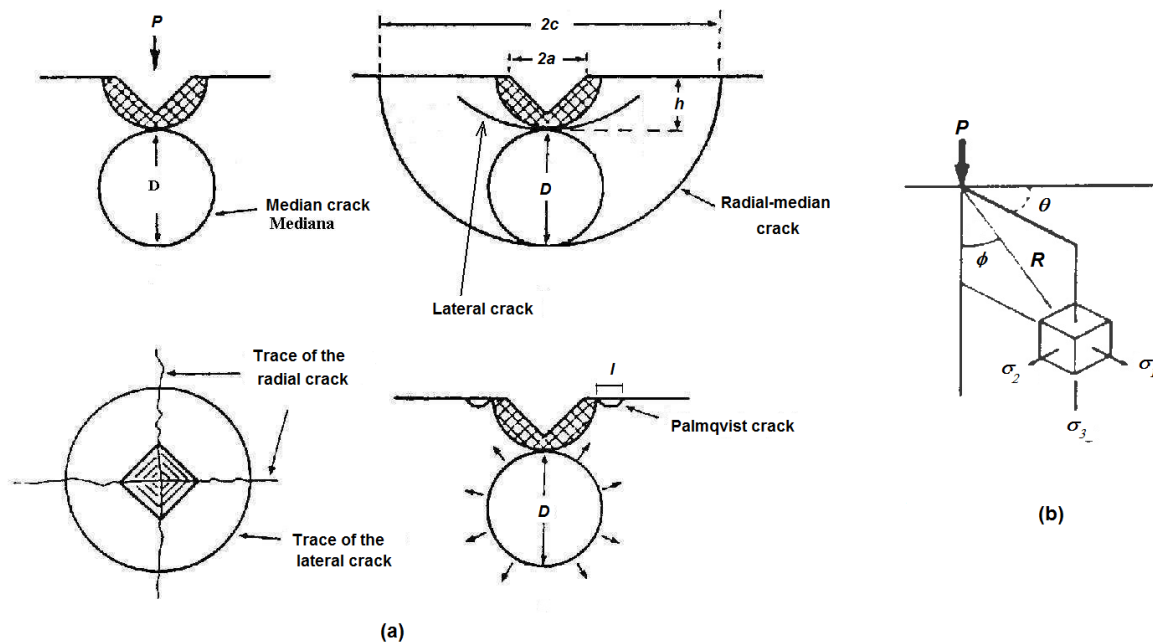


Figure 3. Crack onset during an indentation test (a) Nucleation mechanisms (b) Stress state during loading[9]

2.1.2. The Palmqvist crack

The nucleation of Palmqvist cracks occurs in the interface between plastic deformed elastic regions, but its nucleation point is located close to the sample surface in the diagonal direction of the indenter (Figure 3). The stress state on the surface is similar to that in the case of median crack nucleation, however, faults existing surface may be responsible for stress concentration points that enhance the nucleation of Palmqvist cracks. Acc. to literature cracks on WC-Co alloys are from this type [7, [9].

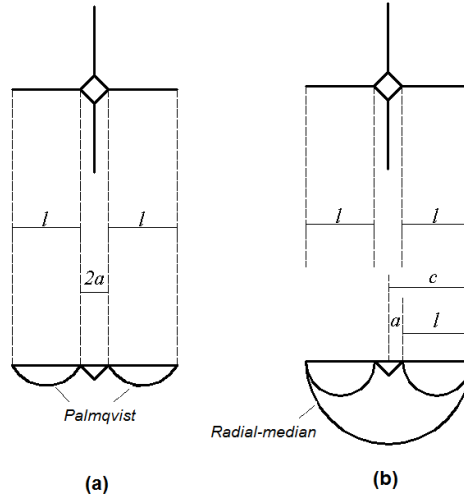


Figure 4. Crack Models (a) Palmqvist; (b) Median [3]

2.1.3. The lateral crack

This crack can propagate from the median crack during the unloading phase, however, parallel to the specimen surface and in the interface of the region of plastic deformation (Figure 3a). This crack is associated with the lateral surface wear in brittle materials during service. However, these crack models are rarely used to evaluate K_{IC} [3].

2.2. Experimental Models for WC-Co K_{IC} Evaluation.

Several research works found semi-empirical methodologies to correlate Young modulus, hardness and fracture toughness with the length of radial cracks during the indentation tests in brittle materials. Since WC-Co alloys have a brittle mechanical behaviour, many efforts were done, in order to find expressions able to determine their material properties. The first who studied these cracks and their potential use by determining fracture toughness was Palmqvist (1963). Working with WC-Co and pyramidal indenter, the author identified an important parameter in the formation of cracks. Later, Evans & Charles (1976) initiated analysis of formation of these cracks in detail. This work culminated in the development of a correlation between the size and shape of the crack, the load and fracture toughness K_{IC} [9]. In 1981, Anstis *et al.* based on experimental tests with various types of ceramic materials, set another expression for the evaluation of K_{IC} considering the a model of crack radial-median. Eq. (2) shows the relationship proposed by Anstis *et al.*, where $\Omega = 0.016 \pm 0.004$, H is Vickers Hardness, E is Young Modulus, P is the applied load and c is the total length of the crack (Figure 4) [9].

$$K_{IC} = \Omega \left(\frac{P}{(c)^{3/2}} \right) * \left(\frac{E}{H} \right)^{1/2} \quad (2)$$

In 1982, Niihara *et al.* found with experimental tests that the radial cracks in the WC-Co would be a Palmqvist for small loads (P). For radial cracks type Palmqvist, he proposed a new equation, where the constant $B_2=0.035$ (indenter form,) and $\phi = 2.7$ (material constant). Eq. (3) is valid for cracks $0.25 < l/a < 2.5$. [9].

In 1983, Niihara reinterpreted that the Palmqvist crack nucleation occurred prior to crack nucleation median. In developing this model, the author found that the superficial radial crack would become semi-elliptical. In this new model, he gave the value to the constant $B_2 = 0.0485$ in eq. (3). [9].

$$K_{IC} = \left(\frac{B_2}{\phi^{0.6}} \right) H a^{1/2} \left(\frac{E}{H} \right)^{0.4} \left(\frac{l}{a} \right)^{-1/2} \quad (3)$$

Later, Szutkowska (1999) called attention to the negative influence of residual stresses due to preparation of test specimen on the results obtained and suggested use of eq. (3) considering $B_2=0.035$ and $\phi = H/\sigma_{YS}$, where σ_{YS} is the yield strength of the material. [10]. In 1985, Shetty *et al.* correlated a semi-empirical expression for K_{IC} (eq. 4) by defining a crack nucleation parameter W (eq. 5). These authors concluded that the radial-median cracks would not occur in WC-Co with cobalt content more than 5% and, in these cases, would always be produced Palmqvist cracks [9].

$$K_{IC} = 0.0937(HW)^{1/2} \tag{5}$$

$$W = P/4l \tag{4}$$

Laugier, in 1985, assumed that the Anstis cracks were type Palmqvist and came to eq. (6). [9]

$$K_{IC} = 0.015 \left(\frac{P}{C^{3/2}} \right) \left(\frac{l}{a} \right)^{-1/2} \left(\frac{E}{H} \right)^{2/3} \tag{6}$$

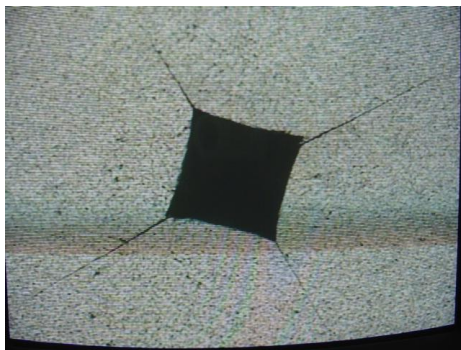
These studies show that this field of research is still being explored and that the use of indentation tests and still raises critics and questions about your application for WC-Co alloys. Although there is a reasonable consensus that the system of cracks that occur for WC-Co is the type Palmqvist, there are still some difficulties to determine the fracture toughness. These aspects are more evident when studying these materials used in surface coatings [10]. In these sense, the application of FE models to study the stress and strain states during the hardness tests can contribute with a better understand on the mechanism of crack nucleation and propagation on the WC-Co.

3. METHODOLOGY

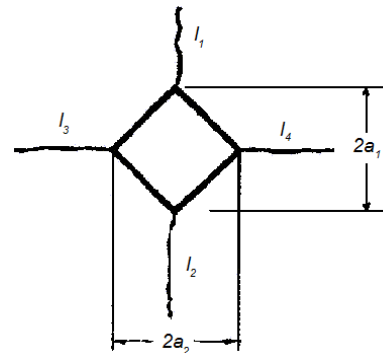
The Vickers test has a very important characteristic from the point of view of numerical simulation. Since the hardness is the ratio between the force and the area of the indenter impression, the load application can be idealized as prescribed displacement instead of the applying force, allowing better control over the cycle number indentation. The present numerical analysis was performed in two phases: loading and unloading.

3.1. Experimental Vickers Hardness Testing

As shown in the previous section, the literature provides several approaches and models to determine fracture toughness of brittle materials through Indentation tests. In order to verify and compare the different expressions and get a better comprehension about the indentation and test methodologies, two WC-Co specimens were prepared and Vickers indentation tests were performed under loads 60 kgf and 120 kgf, respectively. After the indentation, radial cracks appear on the print corners (Figure 5). The diagonals (a_1 and a_2) as well the crack length on the surface were measured and the fracture toughness was evaluated.



(a)



(b)

Figure 5. (a) WC-Co specimen after-Indentation (b) Illustration of the radial cracks

3.2. Numerical Study

In this numerical analysis, the focus of this paper is to study the stress and strain field during the loading phase. The pyramidal Vickers indenter was modeled as a rigid shell penetrating on a flat surface. A quarter-symmetry of the specimen was assumed (Figure 6). Table 3 summarizes the FE mesh, BCs and load application.

Table 2: FE model summary

	Mesh	Boundary Conditions	Loads
Specimen	1800 elements 2191 nodes	Base: constrained in Z Symmetry: constrained in X and Y	n.a.
Indenter	Rigid shell	n.a.	Prescribed displacement $\Delta z = -17\mu\text{m}$ (BEGIN contact) $\Delta z = -70\mu\text{m}$ (END contact) 20 load steps

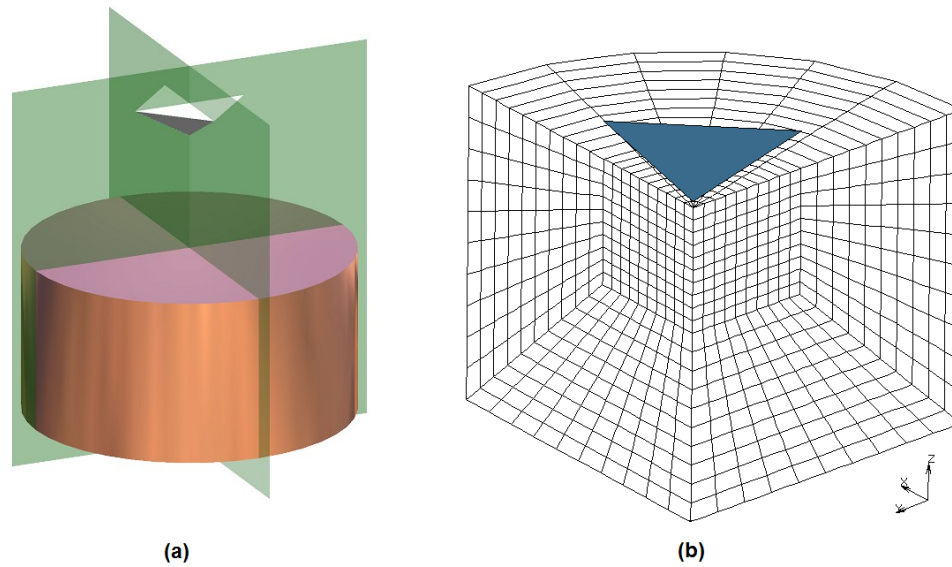


Figure 6. Vickers Testing Idealization (a) Illustration (isometric view) (b) FE Model.

The material studied in these analyzes was the WC-6Co, which shows a mechanical behaviour between brittle and elastic-plastic. For this simulation an elastic-plastic curve based on a power law is assumed to represent the material behaviour. Table 3 summarizes the material properties adopted on this simulation [3, 5].

Table 3: WC-6Co Material Properties[3, 5]

	Young Modulus E [GPa]	Poisson ν	Yield Strength σ_{YS} [MPa]	Stress-strain response $\sigma(\epsilon)$ [MPa]	Fracture Toughness K_{IC} [MN/m ^{3/2}]
WC-6Co	619.5	0.28	5760	$\sigma = 18060 \epsilon^{0.244}$	10.0

4. RESULTS AND DISCUSSIONS

4.1 Experimental Results

Table 4 illustrates the experimental results of Vickers Indentation testing. Based on these test data, the hardness was calculated between 16.02 GPa to 16.38 GPa, what is accordance with typical values funded in the literature [3, 9].

Table 4: Vickers Indentation - Experimental Results

Load (kgf)	Hardness (GPa)	Diagonal (2a)	Radial Crack (l)	l/a
60	16.02	259 μm	293 μm ; 229 μm	2.43
		263 μm	310 μm ; 436 μm	
120	16.38	362 μm	530 μm ; 601 μm	2.53
		368 μm	336 μm ; 381 μm	

Figure 7 shows the fracture toughness for WC-Co calculated for each individual crack (symbols I to IV) and for the mean length crack. Niihara expression (eq. 3) and Szutkowska equation gives reasonable values and are in accordance to conventional fracture toughness tests ($K_{IC} = 10 \text{ MN/m}^{3/2}$, Table 3). It is important to remark that models for Palmqvist cracks are only valid if $0.25 \leq l/a \leq 2.50$. Therefore, it was reasonable to taken into account for calculations, only the results from the test 60kgf ($l/a = 2.43$).

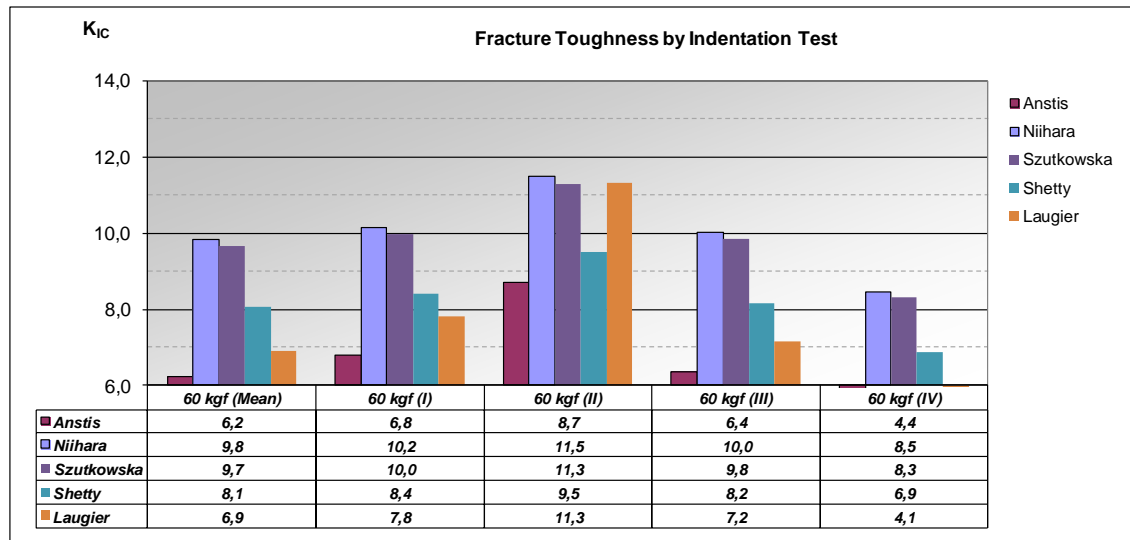


Figure 7. Fracture toughness K_{IC} Calculation (Units in $N/mm^{3/2}$)

4.2 Numerical Results

Figure 8 shows the evolution of the numerical stress field (Von Mises stress) during the indentation test. The indenter (positioned $17\mu m$ over the specimen) begin the simulation from a position $z=0.0$. A prescribed displacement of $\Delta z = -70\mu m$ is applied in 20 steps. The stresses on the contact region increase and a plasticization begins on the surface. Under this region, the stress level increases linearly. Figure 9 shows the stress level in the end of loading phase. It can be observed the highest stress level occurs under the indent print and in the diagonal directions, which can explain the radial after the test. The nucleation of these cracks can be correlated with the residual stresses on the interface between plastic and elastic regions.

5. OVERALL CONCLUSIONS

The analysis by FE model in this research work gives reasonable results for the global behaviour of the Vickers indentation test. Two critical regions can be identified during the loading phase:

I. Along the diagonal: high tensile stress level on this region. Surface plastic strains appear in the end of the loading phase.

II. Under the indention region: Elevation of elastic stresses due to the compression. Plastic strains appear on the region in direct contact with the indenter.

Hence during the loading phase, a crack can nucleates due residual stresses on the region (I), if the load is higher than a critical, in other words, if the Stress Intensity Factor (SIF) is higher than the fracture toughness. The hydrostatic stress state created on region (II) is less critical and even if a crack nucleates, it occurs stably. During the unloading phase, crack nucleation on both regions is expected. Firstly due to residual stress on the interfaces between plastic and elastic regions, which appears due to the relaxation of elastic strains and, of course, due to surface material failures and faults, which can act as a stress concentrator. In a future development of this work, it will be intended to model a Palmqvist radial crack along the indentation diagonal. This crack can assume a semi-elliptical geometry, what is consistent with experimental and numerical results found in the literature for WC-Co [3]. It is expected that this model is capable of providing results for a better understand of the mechanisms of crack growth in WC-6Co indentation tests.

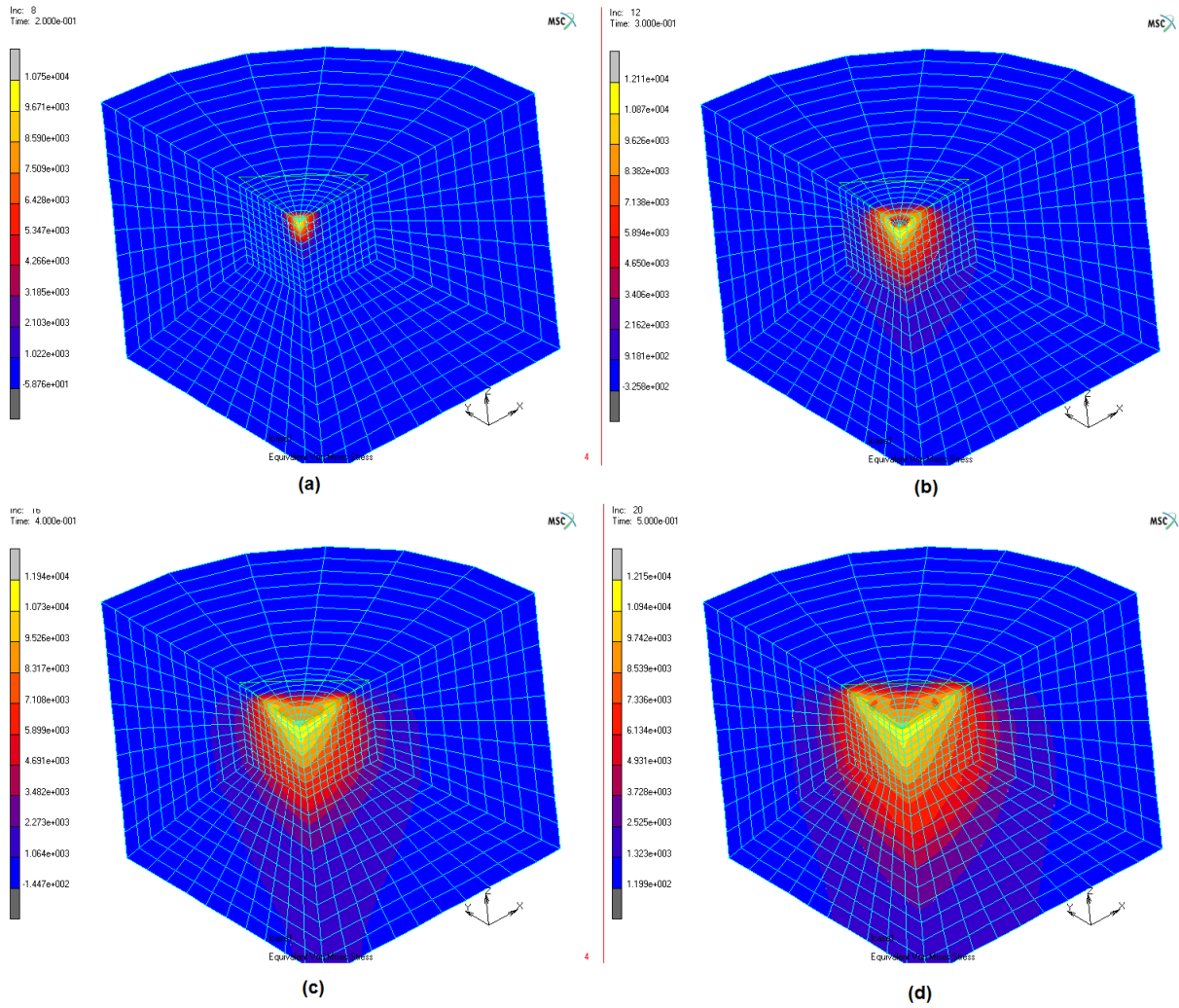


Figure 8. Stress Field during the loading cycle (a) $\Delta z = -28 \mu\text{m}$; (b) $\Delta z = -42 \mu\text{m}$; (c) $\Delta z = -56 \mu\text{m}$; (d) $\Delta z = -70 \mu\text{m}$

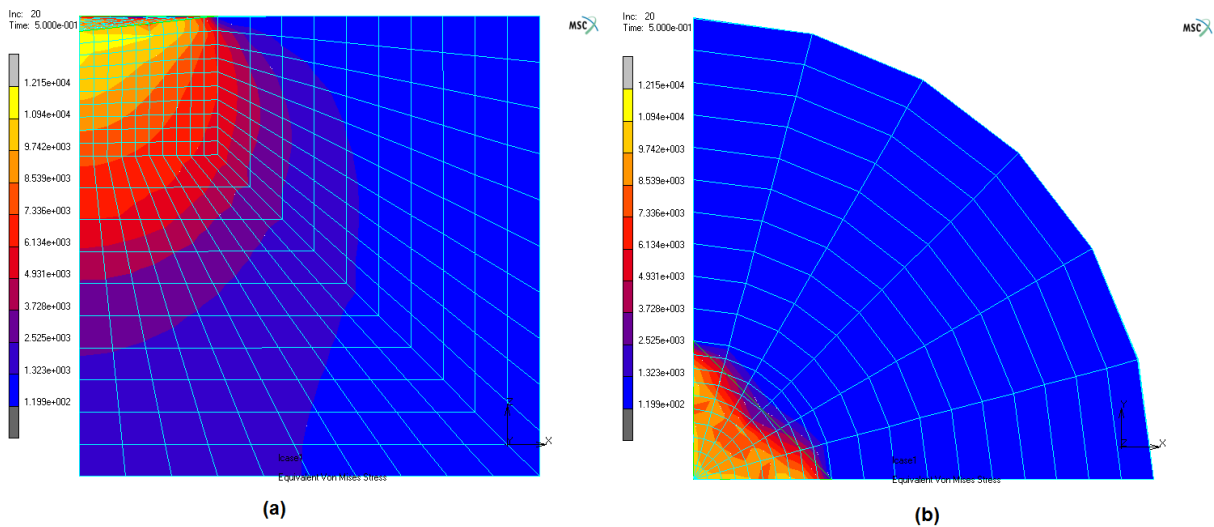


Figure 9. Stress Field at 100% loading (a) front view; (b) top view

6. ACKNOWLEDGEMENTS

The authors thank for the financial and technological support from the CNPq (National Council for Scientific and Technological Development), the FAPEMIG (Foundation for Research Support of Minas Gerais) and UFSJ (Federal University of São João del Rei).

7. REFERENCES

- [1]. Anderson, T. L. "Fracture Mechanics - Fundamentals and Applications". 3rd Ed. CRC Press, Inc., 2005, 688p
- [2]. Donato, G. H. B., Magnabosco, R., Ruggieri, C., Effects of weld strength mismatch on J and CTOD estimation procedure for SE(B) specimens, International Journal of Fracture, 159, issue 1, 1-20, 2009.
- [3]. Dias, A.M.S., "Análise Numérica do Processo de Fratura no Ensaio de Indentação Vickers em uma Liga de Carboneto de Tungstênio com Cobalto", PhD Thesis. Federal University of Minas Gerais, Brazil, 200p, 2004. [in Portuguese]
- [4]. Strecker, K.; Ribeiro, S.; Hoffmann, M. J., Fracture Toughness Measurements of LPS-SiC: A Comparison of the indentation Technique and the SEVNB Method, Materials Research, 8, n. 2, 121-124, 2005.
- [5]. Dias, A. M. S., Modenesi, P. J., Godoy, C., Computer Simulation of Stress Distribution During Vickers Hardness Testing of WC-6Co, Materials Research, 9, n. 1, 73-76, 2006.
- [6]. Dias, A.M.S., Godoy, C., Determination of Stress-Strain Curve through Berkovich Indentation Testing, Materials Science Forum, 636-637, 1186-1193, 2010.
- [7]. Dias, A.M.S., Miranda, J.S., Godoy, G.C., Avaliação da tenacidade à fratura através do ensaio de indentação em pastilhas de metal duro, Matéria, 14, n. 2, 869-877, 2009. [in Portuguese]
- [8]. Zhang, W; Subhash, G., 2001. Finite Element Analysis of Interacting Vickers Indentations on Brittle Materials, Acta Materialia, 49, 2961-2974, 2001.
- [9]. Ponton, C. B., Rawlings, R.D., Vickers Indentation Fracture Toughness Test, Part 1: Review of Literature and Formulation of Standardized Indentation Toughness Equations, Materials Science and Technology, 5, 865-872, 1989.
- [10]. Szutkowska, M., Fracture Toughness Measurement of WC-Co Hard-metals by Indentation Method, Journal of Advanced Materials, 31, 3-7, 1999.
- [11]. Dias, A. M. S., Numerical Study of Spherical Indentation in Superficial Coatings, International Journal of Research and Reviews in Applied Science, 11, 2, 271-278, 2012.
- [12]. Medeiros, E. E., Dias, A. M. S., Christoforo, A. L., Numerical Simulation of Mechanical Fracture Testings, International Journal of Materials Engineering, Vol. 2 No. 5, 2012, pp. 61-66.

APPENDIX

A.1. Review of Fracture Mechanics

In the mechanical fracture analysis, the critical combination of three variables is considered: the applied stress, the size of the crack and the fracture toughness of the material [T. L. Anderson, 2005]. There are three basic modes of loading as shown in Figure A1. The stress intensity factor (K_I , K_{II} , K_{III}) defines the amplitude of the stress singularity at the crack tip and is related to the geometry of the structure and the applied stress. This relationship is defined by Linear Elastic Fracture Mechanics (LEFM) through of eq. (A1).

$$K_{I,II,III} = Y\sigma\sqrt{\pi a} \quad (A1)$$

In this expression, σ is the normal stress, a is the crack length and Y is a shape factor which depends on the loading mode and the geometry of the structure. Already the fracture toughness (K_{IC}) is a mechanical property of the material and indicates a boundary condition of crack propagation in mode I. In the analysis of problems of LEFM, this property has been adopted as a criterion of failure in structures and mechanical components. The assessment of this parameter is performed by ASTM E-399 (1999).

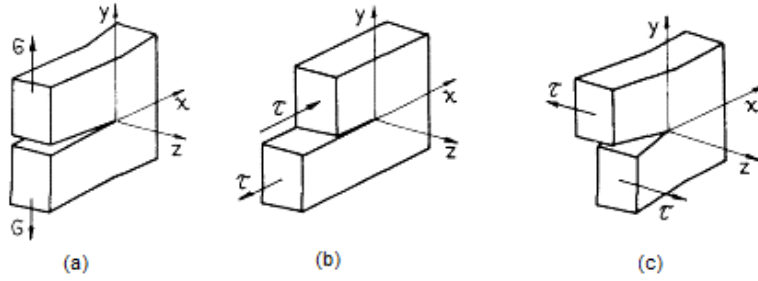


Figure A1. (a) Mode I – tension; (b) Mode II – longitudinal shear; (c) Mode III – transversal shear [Anderson, T. L, 2005].

Another important parameter, commonly used in fracture mechanics, is the *J Integral*. This parameter is related to the energy absorbed by the material, which comprises a component due to elastic strain with the plastic strain. The formulation of the *J Integral* is expressed by eq. (A2), where parameter *w* is the strain energy density, *T_i* are the components of the traction vector, *n_j* are the components of the unit vector *Γ*, *u_i* are components of the deformation vector and *ds* is the incremental length along the trajectory *Γ*, Figure A2.

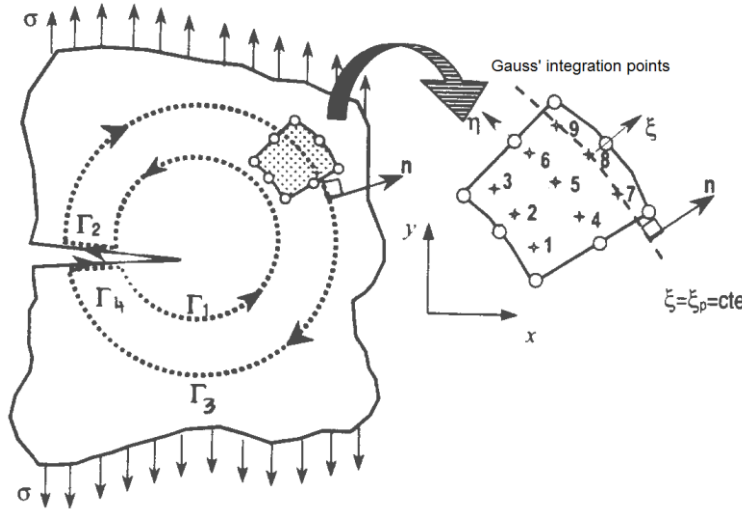


Figure A2. Numerical integration trajectory to evaluate the *J Integral* [Medeiros et al., 2012]

$$J = \int_{\Gamma} \left(w dy - T_i \frac{\partial u_i}{\partial x} ds \right) \tag{A2}$$

The formulation described through equation (A2) to (A4) is not usual for analysis by finite element. There are numerical difficulties due to the definition of integration via a single path *Γ*. In fact, The boundary *J Integral* is converted into a full area defined by paths *Γ₁*; *Γ₂*; *Γ₃* and *Γ*, as shown in Figure A2.

$$w = \int_0^{\epsilon_{ij}} \sigma_{ij} d\epsilon_{ij} \tag{A3}$$

$$T_i = \sigma_{ij} n_j \tag{A4}$$